THE JOURNAL OF PHYSICAL CHEMISTRY C

Article

pubs.acs.org/JPCC

Role of Water and Phase in the Heterogeneous Oxidation of Solid and Aqueous Succinic Acid Aerosol by Hydroxyl Radicals

Man Nin Chan,[†] Haofei Zhang,[†,‡] Allen H. Goldstein,[‡,§,∥] and Kevin R. Wilson*[,†]

[†]Chemical Sciences Division, Lawrence Berkeley National Laboratory, Berkeley, California 94720, United States

[‡]Department of Environmental Science, Policy, and Management, University of California, Berkeley, California 94720, United States

[§]Environmental and Energy Technologies Division, Lawrence Berkeley National Laboratory, Berkeley, California 94720, United States

[∥]Department of Civil and Environmental Engineering, University of California, Berkeley, California 94720, United States

ABSTRACT: The effect of the aerosol phase (solid versus aqueous) on the heterogeneous OH oxidation of succinic acid ($C_4H_6O_4$) is investigated using an aerosol flow tube reactor. The molecular and elemental transformation of the aerosol is quantified using Direct Analysis in Real Time (DART), a soft atmospheric pressure ionization source, coupled to a high-resolution mass spectrometer. The aerosol phase, controlled by liquid water content in the particle, is observed to have a pronounced effect on the reaction kinetics, the distribution of the oxidation products, and the average aerosol carbon oxidation state. In highly concentrated aqueous droplets (~28 M), succinic acid within the aerosol reacts 41 times faster than in solid aerosol, producing a larger quantity of both functionalization and fragmentation reaction products. These observations are consistent with the more rapid diffusion of succinic acid to the surface of aqueous droplets than solid particles. For aqueous droplets at an OH exposure of 2.5×10^{12} molecules cm^{-3} s, the average aerosol carbon oxidation state is +2, with higher molecular weight functionalization products accounting for ~5% and lower carbon number (C < 4) fragmentation products comprising 70% of the aerosol mass. The remaining 25% of the aqueous aerosol is unreacted succinic acid. This is in contrast with solid aerosol, at an equivalent oxidation level, where unreacted succinic acid is the largest aerosol constituent with functionalization products accounting for <1% and fragmentation products ~8% of the aerosol mass, yielding an average aerosol carbon oxidation of only +0.62. On the basis of exact mass measurements of the oxidation products and a proposed reaction mechanism, succinic acid in both phases preferentially reacts with OH to form smaller carbon number monoacids and diacids (e.g., oxalic acid). These results illustrate the importance of water in controlling the rate at which the average aerosol carbon oxidation state evolves through the formation and evolution of C−C bond scission products with high carbon oxidation states and small carbon numbers. These results also point more generally to a potential complexity in aerosol oxidation, whose chemistry may ultimately depend upon the "exposure history" of particles to relative humidity.

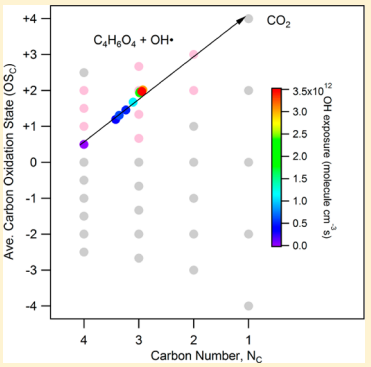

1. INTRODUCTION

Hydrocarbons are a significant fraction of ambient aerosol mass[1] and can continuously undergo oxidation by colliding with gas-phase oxidants such as hydroxyl radicals (OH), ozone (O_3), and nitrate radicals (NO_3) in the atmosphere. The impact of heterogeneous oxidation on the composition and properties of organic aerosol has been reviewed in the recent literature.[2] For example, chemical tracers such as levoglucosan (a tracer for biomass burning) can be efficiently oxidized by OH,[3,4] which may complicate the use of these tracers for source apportionment studies.[5,6] Furthermore, chemically reduced organic aerosol (e.g., long chain alkanes) can become efficient cloud condensation nuclei upon only a few generations of heterogeneous oxidation by OH.[7,8]

A number of previous studies have focused on the oxidation of chemically reduced organic compounds (i.e., linear, branched, or cyclic large hydrocarbons).[5,9−13] These results indicate that the observed OH reaction probability or uptake coefficient (i.e., the inferred fraction of OH−particle collisions that yield a reaction) is larger than ~0.1. In broad terms these heterogeneous reactions occurring on liquid hydrocarbon aerosols proceed statistically[14] both by the formation of new functional groups (termed functionalization) and by the production of more volatile products formed via C−C bond scission reactions (termed fragmentation).[15] Together these reaction pathways can yield complex oxidation trajectories,[8,12,14] for example, when represented in the average aerosol carbon oxidation state vs carbon number space as shown by Kroll et al.[16] For chemically reduced hydrocarbons, the initial stages of oxidation form new alcohol and ketone oxygenated functional groups, while smaller carbon number fragmentation

Special Issue: John C. Hemminger Festschrift

Received: February 3, 2014
Revised: March 3, 2014
Published: March 4, 2014

   dx.doi.org/10.1021/jp5012022 | J. Phys. Chem. C 2014, 118, 28978−28992

products are formed only after multiple generations of oxidation.[12,14,17]

The composition of ambient aerosol is much more complex than simple long-chain hydrocarbons and includes hundreds of different multifunctional organic compounds with a wide range of properties (e.g., polarity, solubility, and volatility).[18,19] Aged ambient organic aerosol always contains a significant fraction of more oxygenated hydrocarbons,[20] and as such their heterogeneous chemistry, due to the presence of existing oxygenated functional groups, may differ significantly from those chemical reduced model compounds studied previously. For example, Kroll et al.[15] and Wilson et al.[14] observed in the multigenerational oxidation of squalane ($C_{30}H_{62}$) that the branching ratio for carbon loss (a marker for fragmentation) depends upon the oxygen-to-carbon (O/C) ratio of the reaction product, which reached a value near unity (fragmentation dominates) for those species with an O/C ratio >0.5.

Recently model compounds that better represent the reactivity of multifunctional oxygenated organic aerosols have been investigated.[3,4,21,22] These studies observed that more oxygenated molecules react heterogeneously with OH radicals with uptake coefficients ranging from 0.37 to 1. In some cases[3,4] (erythritol, levoglucosan, abietic acid, and nitroguaiacol), the production of gas-phase products is observed to be efficient, consistent with an enhancement in the fragmentation pathway for more oxygenated aerosol proxies. Yet, for other model compounds[21] (1,2,3,4-butanetetracarboxylic acid, citric acid, tartaric acid, and Suwannee River fulvic acid) the heterogeneous reaction exhibits nonexponential reaction kinetics (i.e., slowing of the reaction with increasing oxidation), accompanied by minimal mass loss (i.e., fragmentation) despite an increase in the average aerosol carbon oxidation state. In these previous studies of more water-soluble oxygenated aerosol proxies, which are all performed at relatively low relative humidity (<30%), complexity arises due to the possible role of water in controlling either the reaction pathways and/or transport properties of molecules in the aerosol phase.

A number of recent studies have clearly demonstrated that the aerosol phase (solid or liquid) can play an important role in the heterogeneous reaction mechanism and the chemical evolution of the oxidation products.[17,23−25] Aqueous droplets (or deliquescent aerosols) have been frequently detected[26,27] indicating that water is an important constituent of the aerosol phase. Furthermore, water is expected to play a large role in governing the diffusivity of molecules within the aerosol, in much the same way as polymeric materials.[28] Although a few studies have explicitly investigated the effect of water in the aqueous droplets on the heterogeneous chemistry, in general it remains somewhat unclear how the presence of water either enhances or inhibits reactivity.[11,29−31] For example, Gallimore et al.[31] observed that the reaction rate and product distribution were highly dependent upon relative humidity for the reaction of ozone with maleic acid aerosol. Furthermore, water in the aerosol phase or in aqueous droplets may solvate oxidation products, thus enhancing partitioning of materials to the aerosol phase.

Here succinic acid in both solid and aqueous aerosols is used to investigate how phase (controlled here by the aerosol water content) controls the rate of heterogeneous oxidation. An additional goal of this study is to understand how the underlying distribution of molecular species, their carbon oxidation states, and carbon numbers ultimately control how oxidation alters average aerosol elemental composition during a heterogeneous reaction. The reaction products, oxidation states, and carbon numbers are identified using an atmospheric pressure aerosol soft ionization source (Direct Analysis in Real Time, DART)[32,33] coupled with high-resolution mass spectrometry. Succinic acid, whose properties are shown in Table 1, is chosen as a model compound for dicarboxylic acids and more generally small water-soluble oxygenated organic compounds. Furthermore, dicarboxylic acids are an important class of organic compounds found in significant concentrations in ambient aerosol.[34]

Table 1. Properties, Rate Constants, and Reactive OH Uptake Coefficients of Succinic Acid

chemical formula	$C_4H_6O_4$
oxygen-to-carbon ratio, O/C	1
hydrogen-to-carbon ratio, H/C	1.5
carbon oxidation state, OS_C	0.5
carbon number, N_C	4
Rate constant, k (cm^3 $molecule^{-1}$ s^{-1})	$2.20 \pm 0.20 \times 10^{-14}$ (solid)
	$1.23 \pm 0.40 \times 10^{-13}$ (aqueous)
reactive OH uptake coefficient, γ	0.04 (solid)
	1.65 (aqueous)

2. EXPERIMENT

2.1. Heterogeneous OH Oxidation. An atmospheric pressure aerosol flow tube reactor is used to investigate the OH initiated heterogeneous oxidation of succinic acid aerosol in the solid and aqueous phases. The experimental details have been described elsewhere.[13,35] Briefly, solid aerosols are generated by atomizing an aqueous succinic acid solution (1 g/L) using a constant output atomizer (TSI Inc. model 3076) and passing the resulting droplet stream through a diffusion drier. The relative humidity (RH) measured at the end of the diffusion drier is less than 10%, which is below the efflorescence point (RH = 55.0−60.2%) of succinic acid.[36] Alternatively, aqueous droplets are formed by removing the diffusion dryer and allowing the aqueous droplets to be directly mixed with humidified nitrogen (N_2), oxygen (O_2), and O_3 before introduction into the flow reactor. After mixing, the RH and temperature inside the aerosol flow tube reactor are 63.8 ± 2.6% and 32.0 ± 0.6 °C, respectively. Since the RH inside the reaction system is always kept higher than the efflorescence point, it is very likely that the succinic acid aerosol exists as aqueous droplets prior to oxidation. At RH = 63%, the aqueous succinic acid droplets are highly concentrated and have a mass fraction of solute of about 0.77 (about 28.4 M).[36] Before oxidation, the size distribution of the aerosol leaving the flow reactor is measured using a scanning mobility particle sizer (SMPS, TSI, Inc.). The mean surface weighted diameter for the solid aerosol distribution is 222.8 ± 0.5 nm with a geometric standard deviation of 1.7. The mean surface-weighted diameter for the aqueous droplet distribution is 154.6 ± 0.7 nm with a geometric standard deviation of 1.5.

The succinic acid aerosol is oxidized by OH radicals, which are generated by the photolysis of O_3 in the presence of water vapor using ultraviolet lamps at 254 nm. The OH concentration is controlled by changing the O_3 concentration and is quantified by measuring the decay of a gas-phase tracer, hexane, using a gas chromatograph. The OH exposure (OH concentration × reaction time) ranges from 0 to 3.5×10^{12} molecules cm^{-3} s. After oxidation, a portion of the aerosol

dx.doi.org/10.1021/jp5012022 | J. Phys. Chem. C 2014, 118, 28978−28992

stream exiting the reactor is sampled into the SMPS for the aerosol size measurement. The remaining flow is introduced into an ionization region of the mass spectrometer. This region is an open space between a soft atmospheric pressure ion source (DART) and the mass spectrometer inlet as described by Chan et al.[32]

2.2. Aerosol-DART Mass Spectrometry. Aerosol mass spectrometry[32,33] measurements are conducted using a DART ionization source (IonSense: DART SVP) interfaced to an Orbitrap Q Exactive (Thermo Scientific) mass spectrometer via a Vapur (IonSense) vacuum interface. In all experiments, the DART ion source and mass spectrometer are operated in negative ionization mode. Helium is used as the ionizing gas at a flow rate of 2 L/min. The desorption angle (the angle of the ion source relative to the MS inlet) and desorption distance (the distance between the orifice of the ion source and the MS inlet) are set to be 45° and 1.5 cm, respectively. The internal DART heater temperature is set at 500 °C, which produces an air temperature in the middle of the ionization region of about 70 °C. This experimental configuration and conditions allow for efficient ion generation and detection.[32] Here all measurements are conducted to measure the bulk composition of the aerosol. To do this, the aerosol stream exiting the flow tube reactor is passed through a stainless steel tube heater (0.25″ diameter and ~6.3″ long), maintained at a temperature of 300 °C. The temperature and aerosol residence time in the heater are sufficient to completely vaporize the aerosol before detection by the mass spectrometer. The resulting gas-phase molecules exiting the heater are directed into the ionization region, where they are ionized by the reactive species in the DART ion source.

The observed ions in the DART aerosol mass spectra, described in detail below, can be explained by the following ionization mechanisms proposed by Cody et al.[37,38] In the negative ionization mode, the electrons (e^-) produced by Penning ionization in the DART ion source are captured by atmospheric O_2 to produce anions (O_2^-) (eq 1). The O_2^- then reacts with gas-phase species (M) thermally desorbed from the aerosol through proton abstraction to yield deprotonated molecular ions, $[M - H]^-$ (eq 2).

$$e^- + O_2(g) \rightarrow O_2^-(g) \quad (1)$$

$$O_2^-(g) + M(g) \rightarrow [M - H]^-(g) + HO_2^{\cdot}(g) \quad (2)$$

In previous studies, it was demonstrated that monoacids (e.g., oleic acid) and dicarboxylic acids (e.g., succinic acid, adipic acid, and suberic acid) can be detected by DART in negative ion mode.[32,33] In this work, the oxidation products are likely comprised of one or two carboxylic acid functional group(s), which would be similarly detected as $[M - H]^-$. Quantifying the aerosol composition from analysis of the DART mass spectra requires a correction of the ionization efficiency of potential oxidation products (e.g., oxalic acid, malonic acid, malic acid, oxosuccinic acid, and tartaric acid). The ionization efficiency of these compounds was measured using authentic standards. The measured ionization efficiency of oxalic acid, malonic acid, oxosuccinic acid, and tartaric acid relative to succinic acid is measured to be 0.5, 0.55, 4.59, and 2.66, respectively. The tartaric acid standard is used to correct the ionization efficiency of the other C4 functionalization products, where authentic standards are not available. Oxalic acid (C_2 dicarboxylic acid) and malonic acid (C_3 dicarboxylic acid) are used to correct the ionization efficiencies for C_2 and C_3 fragmentation products, respectively. Oxalic acid, a C_2 dicarboxylic acid, is detected as $[M - H]^-$, suggesting more generally that the hydrogen (H) atom from one of the carboxylic acid functional groups is abstracted by O_2^- to produce $[M - H]^-$.

For the Orbitrap mass spectrometer, the scan parameters are: the m/z scan range was 70−700 with all spectra recorded at 1 s intervals. The automatic gain control, the desired number of ions in the trap, was set to be 1×10^6 with a maximum injection time of 200 ms. The temperature of the capillary tube is maintained at 200 °C. Each mass spectrum was averaged over a 5 min sampling time with a mass resolution of 140 000. The mass spectra are analyzed using the Xcalibar. Mass calibration is performed by introducing an ion calibration mixture solution (Pierce ESI negative ion calibration, 10 mL, Thermo Scientific) through a small capillary tube at a flow rate of 5 μL/min into the ionization region. The aliquot of the solution at the tip of the capillary tube is vaporized by the DART ion source. The thermally desorbed calibrants are then ionized by the DART source.

3. RESULTS AND DISCUSSION

The following sections are organized as follows: First, the DART mass spectra of the heterogeneous OH oxidation of succinic acid aerosol in solid and aqueous phases are analyzed and the molecular formula of the reaction products assigned (Section 3.1). Second, the oxidation kinetics of solid and aqueous succinic acid aerosol are presented to determine how the oxidation rate depends upon the aerosol phase (Section 3.2). This section is followed by a proposed reaction mechanism combined with the product evolution kinetics to explain how the observed reaction products are formed (Section 3.3). Finally, the average aerosol elemental composition (e.g., oxygen-to-carbon ratio of the particle) is computed from the speciated aerosol measurements, to elucidate how the distribution of molecular products evolve with reaction and ultimately explain the observed oxidation trajectory in the average aerosol carbon oxidation state vs carbon number space[16] (Section 3.4).

3.1. Oxidation Products Detected in DART Mass Spectra. Figure 1 shows the DART mass spectra for the reaction of OH with solid succinic acid aerosol. Before

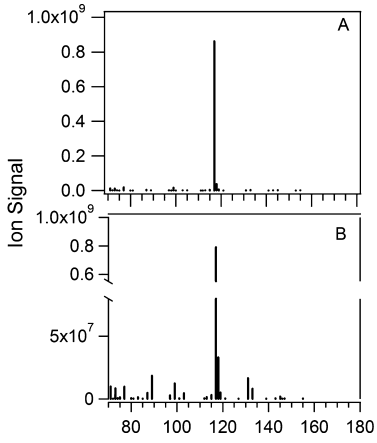

Figure 1. DART mass spectra of solid succinic acid aerosols (A) before oxidation and (B) after oxidation at the OH exposure = 3.3×10^{12} molecules cm^{-3} s. Note that the y-axis in (B) is split to better show the small number of oxidation products.

dx.doi.org/10.1021/jp5012022 | J. Phys. Chem. C 2014, 118, 28978−28992

oxidation (Figure 1A), the deprotonated molecular ion peak ($[M - H]^-$) of succinic acid (m/z = 117) is the dominant ion. Peaks in the mass spectra that indicate decomposition or oxidation of the succinic acid within the ion source itself are not observed. Upon oxidation at an OH exposure of 3.3 × 10^{12} molecules cm^{-3} s (Figure 1B), the succinic acid remains the dominant ion in the mass spectrum. Ions with m/z values smaller and larger than the deprotonated succinic acid ion are observed, albeit in small amounts, with their normalized abundance relative to succinic acid of less than a few percent.

The mass spectra for the OH reaction of aqueous succinic acid droplets are shown in Figure 2. Before oxidation (Figure 2A), as for the solid aerosol, the mass spectrum exhibits a strong deprotonated molecular ion peak. These results suggest that the ionization pathways are very similar for both aerosol phases and independent of water content in the aerosol, as was previously observed by Chan et al.[32] Unlike the solid aerosol, the aqueous droplets undergo a larger change when exposed to OH, as shown in Figure 2B. At an OH exposure of about 2.5 × 10^{12} molecules cm^{-3} s, ∼ 75% of the succinic acid is consumed, accompanied by the appearance of both larger and smaller molecular weight oxidation products in significant amounts.

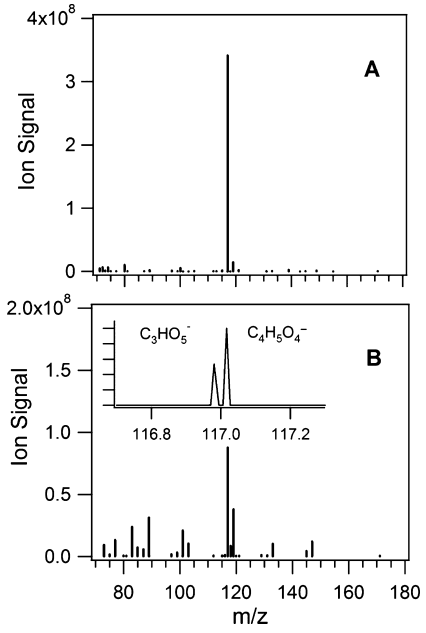

Figure 2. DART mass spectra of aqueous succinic acid droplets (A) before oxidation and (B) after oxidation at OH exposure = 2.5 × 10^{12} molecules cm^{-3} s. (Inset) Expanded region around m/z = 117 showing both succinic acid and a fragmentation product at the same nominal mass.

Tables 2 and 3 summarize the ions that are detected in the DART mass spectrum and their corresponding oxidation products for both solid aerosol and aqueous droplets. A mass tolerance is set to less than ±5 mDa for assigning the chemical formula of the detected ions. On the basis of the detected ions and chemical formulas, the oxidation products that are detected can be broadly classified into two main categories: functionalization and fragmentation products. Functionalization products, shown in Table 2, are formed via the addition of one or two oxygenated functional groups to the C4 carbon backbone of succinic acid. Alternatively, fragmentation products (Table 3) are those oxidation products that have a carbon number less than 4, which are formed by the scission of a C−C bond in the parent succinic acid molecule. Ions with m/z larger than 200 are not observed, suggesting that oligomers, if formed, are below the detection limit of the mass spectrometer. It also cannot be ruled out that some oligomers may thermally decompose during the analysis to yield the fragmentation products with m/z less than 200.

In general, the oxidation products shown in Tables 2 and 3 are consistent with reactions (described in detail below) that form alcohol and carbonyl functional groups. In principle, organic peroxides (ROORs) and hydroperoxides (ROOHs) could possibly be formed by reactions between peroxy radicals and/or hydroperoxy radicals. However, these peroxides, if formed, are expected to thermally decompose in the DART source. However, we find no evidence in the mass spectrum of any fragment ions consistent with the thermal decomposition of these peroxide species.

Overall, there are similarities in the oxidation products detected in both aerosol phases, except those oxidation products with the chemical formula of $C_4H_6O_6$, which only appear in the mass spectra of the aqueous droplets. The abundance of reaction products is much larger in aqueous droplets (Figure 2) than in solid aerosol (Figure 1).

3.2. Oxidation Kinetics of Succinic Acid and Reactive OH Uptake Coefficient. Figures 3 and 4 show the decay of succinic acid as a function of OH exposure in both the solid and aqueous phases. For the solid aerosol, shown in Figure 3A, succinic acid decreases slightly with increasing OH exposure. The succinic acid decays linearly over the reaction and contributes more than 90% of the total ion signal from the particle at the highest OH exposures (3.5× 10^{12} molecules cm^{-3} s) accessed in the experiment. The decay in succinic acid closely resembles the changes in aerosol volume measured by the SMPS and also shown in Figure 3A. The aerosol volume decreases by ∼20% over the course of the reaction. Since the particle is mostly comprised of succinic acid, we do not expect the heterogeneous reaction to produce significant changes in the average aerosol density or shape. As such the decrease in aerosol volume is a reasonable proxy for aerosol mass, suggesting that as the reaction proceeds some gas-phase products are formed and evaporate from the particle (i.e., volatilization), thus leading to a decrease in aerosol volume. The decay in succinic acid and aerosol volume is accompanied by the slow rise in both functionalization (Figure 3B) and fragmentation (Figure 3C) products. The sum of both the fragmentation and functionalization products is shown in Figure 3D. A more detailed analysis of the oxidation products will be conducted below.

In aqueous droplets (Figure 4A), succinic acid decays rapidly at low OH exposures while remaining somewhat unchanged for OH exposures in excess of 1.5 × 10^{12} molecules cm^{-3} s. 25% of the succinic acid remains in the particle at the highest OH exposure (about 2.5 × 10^{12} molecules cm^{-3} s). Also shown in Figure 4A is the aerosol volume measured by the SMPS. Overall, the aerosol volume shows kinetic behavior similar to the succinic acid ion signal, exhibiting a rapid initial decrease followed by a plateau at OH exposures in excess of 1.0 × 10^{12} molecules cm^{-3} s. At the end of the reaction, the measured aerosol volume decreased by about 28% relative to aqueous succinic acid. The point in the reaction (OH exposure = 0.5−1.0 × 10^{12} molecules cm^{-3} s) where the succinic acid and aerosol volume appear to stop reacting with OH coincides with the production of the largest quantity of functionalization

dx.doi.org/10.1021/jp5012022 | J. Phys. Chem. C 2014, 118, 28978−28992

Table 2. Functionalization Products Detected by DART in the Negative Ion Mode in the Series of Heterogeneous OH Oxidation of Succinic Acid Experiments

Suggested compound (Product ID)	Chemical formula	Molecular weight	O/C	H/C	OS_C	Product generation (or Scheme)	Proposed chemical structure
Malic Acid (Funct 1)	$C_4H_6O_5$	134.0132	1.25	1.5	1	1	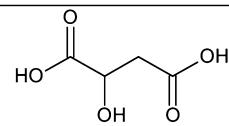
Oxosuccinic acid (Funct 2)	$C_4H_4O_5$	131.9975	1.25	1	1.5	1	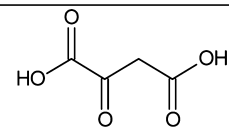
Tartaric acid (Funct 3)[a]	$C_4H_6O_6$	150.0081	1.5	1.5	1.5	2	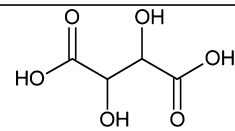
2-hydroxy-3-oxosuccinic acid (Funct 4)	$C_4H_4O_6$	147.9924	1.5	1	2	2	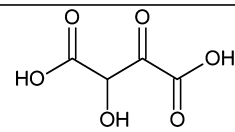
2-hydroxy-2-oxosuccinic acid (Funct 5)[a]	$C_4H_6O_6$	150.0081	1.5	1.5	1.5	2	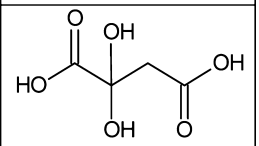

[a]The compound is only detected in the heterogeneous OH oxidation of aqueous succinic acid droplets. Oxidation products are detected as their deprotonated molecular ions, $[M - H]^-$, by DART in negative ion mode. Accurate mass measurements are within ±5 mDa of the theoretical mass associated with the proposed chemical formula for each observed ion.

reaction products (Figure 4B). The fragmentation products rise more slowly (Figure 4C) and reach a maximum at larger exposures than the functionalization products shown in Figure 4B. Figure 4D shows the kinetic evolution of the total functionalization and fragmentation products as a function of OH exposure.

The nonexponential decay kinetics (i.e., an exponential that does not decay to zero) is similar to previous measurements of chemically reduced and more oxygenated model compounds (generally solids) and could originate, as noted previously, from a number of changes in the aerosol produced by free radical oxidation.[3,9,17,21,35] The slowing of the reaction with OH exposure may be due to evolving mass transfer limitations within the aerosol or changes in the viscosity induced by the heterogeneous reaction. This in turn limits the rate at which succinic acid could diffuse from the interior of the particle to the surface for reaction with OH. For example, it could also be possible that the formation of oxidation products changes the composition of the aqueous aerosol enough to induce a phase change such as efflorescence. In this case, the decay kinetics would slow and exhibit an oxidation rate similar to that observed for solid succinic acid described above.

Succinic acid initially decays much faster in aqueous droplets than in solid aerosols. This difference is consistent with the higher mobility of succinic acid and its oxidation products in the aqueous phase. In other words, this more rapid diffusion of molecules from the bulk to the surface leads to the overall oxidation of a larger fraction of the total aerosol volume. For the case where transport is governed solely by molecular diffusion in the particle, the characteristic mixing time (τ) can be roughly estimated as: $\tau = D_p^2/4\pi^2 D$, where D_p is the aerosol diameter and D is diffusion coefficient. The self-diffusion coefficient of organic compounds in different phases (solid, semisolid, and liquid) can vary by orders of magnitudes.[39] Typical diffusion coefficients of organic molecules in solid and liquid phases are $\sim 10^{-20}$ and $\sim 10^{-5}$ cm^2 s^{-1},[39,40] respectively. Although the diffusion coefficient for succinic acid in the solid and aqueous phases is not known, τ is expected to be many orders of magnitude smaller for the solid aerosol. From the diffusion coefficients shown above a rough estimate τ in the solid aerosol and aqueous droplets is 156 years and 3 μs, respectively. This suggests that succinic acid and its oxidation products are much more mobile in aqueous droplets, while in the solid aerosol the oxidation products, once formed, likely remain confined near the surface. This would also imply that replenishment of molecules at the aerosol surface could occur via two very difference mechanisms: volatilization (production of gas-phase reaction products) for uncovering new material at solid interfaces and diffusion of bulk molecules to the surface of aqueous droplets. For example, the changes in aerosol volume observed for solid succinic acid aerosol (Figure 3A) are consistent with some degree of volatilization.

dx.doi.org/10.1021/jp5012022 | J. Phys. Chem. C 2014, 118, 28978−28992

Table 3. Fragmentation Products Detected by DART in the Negative Ion Mode in the Series of Heterogeneous OH Oxidation of Succinic Acid Experiments[a]

Suggested compound (Product ID)	Chemical formula	Molecular weight	O/C	H/C	OS_C	Product generation (or Scheme)	Proposed chemical structure
Glyoxylic acid (Frag 1)	$C_2H_2O_3$	73.9920	1.5	1	2	1, 2, 3	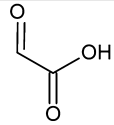
3-oxopropanoic acid (Frag 2)	$C_3H_4O_3$	88.0077	1	1.33	0.67	1	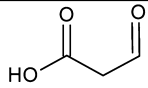
2-hydroxy-3-oxopropanoic acid (Frag 3)	$C_3H_4O_4$	104.0026	1.33	1.33	1.33	2	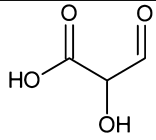
Oxalic acid (Frag 4)	$C_2H_2O_4$	89.9869	2	1	3	2, 3	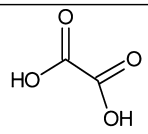
Malonic acid (Frag 5)	$C_3H_4O_4$	104.0026	1.33	1.33	1.33	2	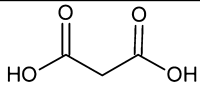
2,3-dioxopropanoic acid (Frag 6)	$C_3H_2O_4$	101.9869	1.33	0.67	2	2	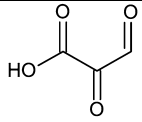
2,2-dihydroxy-3-oxopropanoic acid (Frag 7)	$C_3H_4O_5$	119.9975	1.67	1.33	2	3	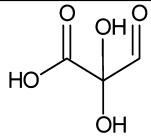
Hydroxymalonic acid (Frag 8)	$C_3H_4O_5$	119.9975	1.67	1.33	2	3	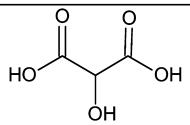
Oxomalonic acid (Frag 9)	$C_3H_2O_5$	117.9818	1.67	0.67	2.67	3	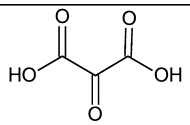

[a]Oxidation products are detected as their deprotonated molecular ions, $[M - H]^-$, by DART in negative ion mode. Accurate mass measurements are within ±5 mDa of the theoretical mass associated with the proposed chemical formula for each observed ion.

From the data alone, we cannot rule out that the large difference in the reactivity of solid and liquid aerosol may also be due, in part, to the more efficient sticking of gas-phase OH radicals to the surface of aqueous droplets, presumably due to enhanced hydrogen bonding to water. For example, Nájera et al.[30] pointed out that the O_3 trapping ability of the aerosol surface is enhanced due to the presence of water and organic acids in aqueous droplets. This in turn could lead to an increase in the overall reaction rate in the aqueous droplets, resulting in higher product yields.[29,30]

To estimate the difference between the reactivity of solid and aqueous aerosol, the observed rate for the OH oxidation of succinic acid is

$$-\frac{d[\text{Succinic}]}{dt} = k[\text{OH}][\text{Succinic}] \quad (3)$$

$$\frac{[\text{Succinic}]_t}{[\text{Succinic}]_0} = e^{-k[\text{OH}]t} \quad (4)$$

where k is the apparent reaction rate coefficient. $[\text{Succinic}]_0$ and $[\text{Succinic}]_t$ are the initial succinic acid concentration and

dx.doi.org/10.1021/jp5012022 | J. Phys. Chem. C 2014, 118, 28978−28992

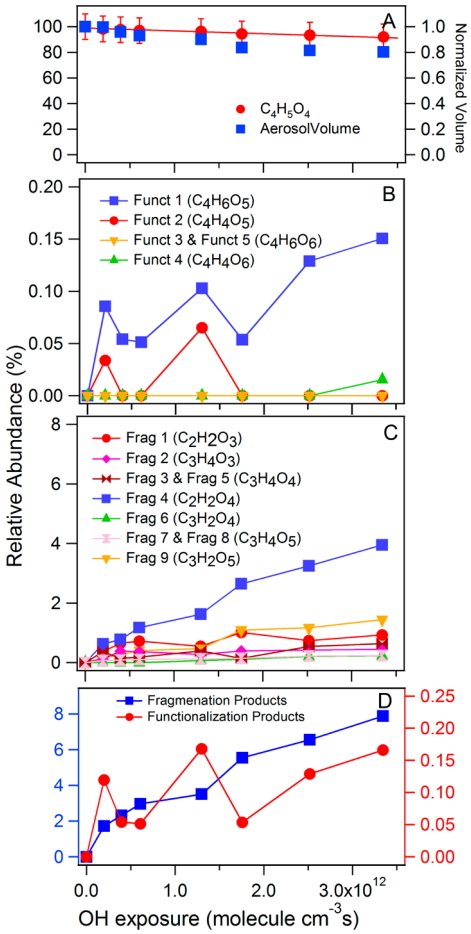

Figure 3. Chemical evolution of solid succinic acid aerosol. (A) The chemical evolution of succinic acid and aerosol volume. Evolution of the (B) functionalization and (C) fragmentation reaction products in the solid aerosol as a function of OH exposure. (D) The total quantity of functionalization and fragmentation products as a function of OH exposure.

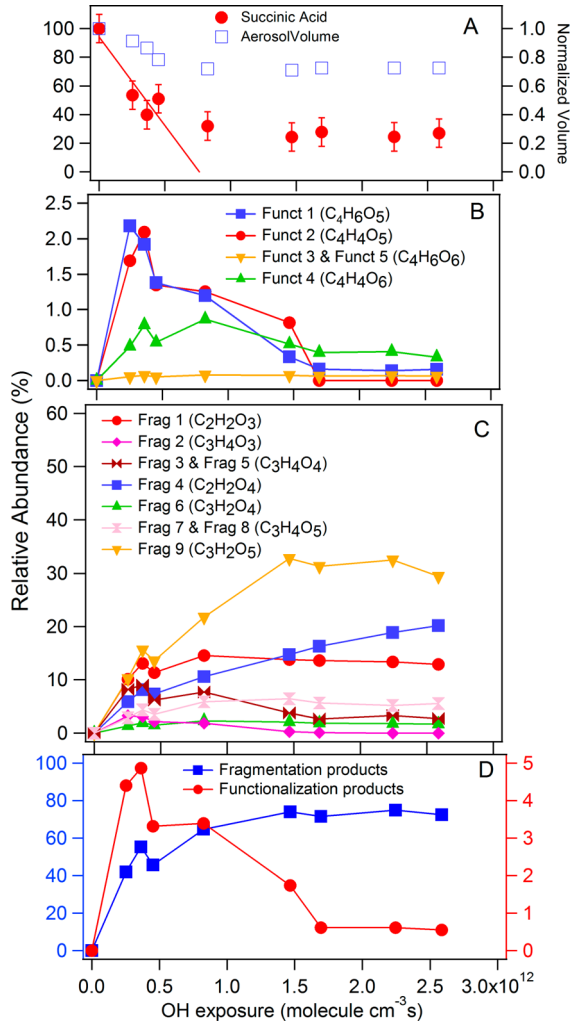

Figure 4. Chemical evolution of aqueous succinic acid droplets. (A) The chemical evolution of succinic acid and aerosol volume. Evolution of the (B) functionalization and (C) fragmentation reaction products in the aqueous aerosol as a function of OH exposure. (D) The total quantity of functionalization and fragmentation products as a function of OH exposure.

succinic acid concentration at reaction time t, respectively. $[OH]t$ is the OH exposure. Nonexponential decay kinetics have been previously observed[3,4,11,35] in a number of heterogeneous reactions on solid aerosols. As shown by Kessler et al.[3] and others,[9,35] a linear fit to the initial decay (i.e., "initial rate analysis") of the reactant, where the aerosol is comprised mostly of succinic acid, can provide a rough estimate of k in the case where the kinetics are nonexponential.[9] The rate constants determined in this way, for solid aerosol and aqueous droplets, are $2.20 \pm 0.20 \times 10^{-14}$ cm^3 $molecule^{-1}$ s^{-1} and $1.23 \pm 0.40 \times 10^{-13}$ cm^3 $molecule^{-1}$ s^{-1}, respectively (Table 1).

From k, the OH reactive uptake coefficient, γ, defined as the fraction of OH collisions that produce a reaction, can also be estimated[13] via

$$\gamma = \frac{4kD_p\rho N_A}{6\bar{c}M_w} \quad (5)$$

where D_p is the mean surface weighted aerosol diameter; ρ is the density of succinic acid; N_A is Avogadro's number; $\bar{c}$ is the average speed of OH radicals; and M_w is the molecular weight of succinic acid. The density of the aqueous droplets is assumed to be the same as that of aqueous succinic acid. From the initial rate analysis, the reactive OH uptake coefficients for solid aerosol and aqueous droplets are estimated to be 0.04 and 1.65, respectively. An uptake coefficient larger than unity implies secondary chemistry, which will be discussed in more detail below. In general, on average the aqueous droplet is ~41 times more reactive than the solid aerosol. It should be noted that this difference in reactivity appears entirely driven by the more rapid replenishment of succinic acid to the surface of the aqueous droplet rather than any fundamental difference in the elementary OH + succinic acid rate coefficient.

3.3. General Reaction Mechanism. Using the exact mass of the product ions detected in the mass spectra and the heterogeneous OH oxidation pathways previously published,[9,10,34,41,42] Figure 5 summarizes the general reaction pathways that are proposed to explain the formation of the observed reaction products in both phases (Tables 2 and 3). The reaction pathways, shown in Figure 5, can be broadly divided into two main categories: functionalization and fragmentation. For functionalization, reaction pathways (**R1**–**R4**) increase the molecular weight by the addition of carbonyl and alcohol functional groups to the C4 carbon backbone of succinic acid. For the fragmentation, more volatile oxidation

dx.doi.org/10.1021/jp5012022 | J. Phys. Chem. C 2014, 118, 28978–28992

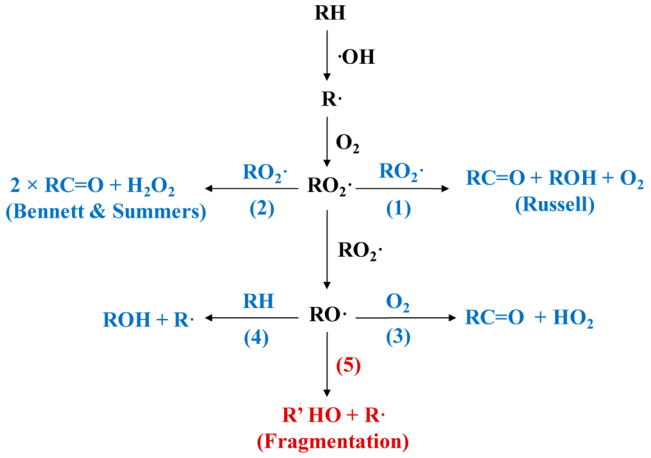

Figure 5. General reaction pathways for the OH oxidation of hydrocarbons (RH) that are used to explain the formation of observed succinic acid oxidation products in the solid and aqueous phases. The functionalization processes are highlighted in blue, and the fragmentation process is highlighted in red.

products with carbon numbers smaller than the parent molecule are formed via the β-scission of an alkoxy radical (**R5**). All of the detected reaction products can be best explained by the well-known Russell (**R1**), Bennett and Summers (**R2**), and alkoxy radical reaction pathways (**R3**–**R5**). As noted above, an OH uptake coefficient larger than 1 is observed for aqueous droplets, suggesting radical chain chemistry. Given the clear importance of alkoxy radicals in this system (as will be demonstrated below), it appears likely that radical chain propagation could proceed via an intermolecular hydrogen abstraction reaction by RO• (**R4**) as recently observed by Ruehl et al.[17] These generalized reaction pathways form the basic chemistry used in the explicit reaction schemes shown in Figures 6–8 for the multigenerational oxidation of succinic acid described below.

3.3.1. First-Generation Products. Figure 6 shows the proposed formation mechanism of first-generation products from the reaction of OH with succinic acid. The products shown in boxes in Figure 6 are molecules consistent with the ions detected in the mass spectrum and shown in Tables 1 and 2. First-generation products are formed via a single H abstraction reaction of OH at one of the four aliphatic hydrogen positions of succinic acid, thus forming an alkyl radical. The alkyl radical quickly reacts with O_2 to form a peroxy radical. The self-reaction of two peroxy radicals (**R1**, Figure 5) can form two functionalization products: malic acid (Funct 1) and oxosuccinic acid (Funct 2). The self-reaction of two peroxy radicals can also produce two alkoxy radicals, which undergo β-scission (**R5**, Figure 5) to yield one C_2 (glyoxylic acid, Frag 1) and one C_3 fragmentation product (3-oxopropanoic acid, Frag 2), which are consistent with the observed ion peaks in the DART mass spectra (see Tables 1 and 2). Malic acid (Funct 1) and oxosuccinic acid (Funct 2) can also be formed directly from alkoxy radical reactions: malic acid (Funct 1) from intermolecular H atom abstraction (secondary chemistry) and oxosuccinic acid (Funct 2) via reaction with O_2. The formation of malic and oxosuccinic acid by either peroxy or alkoxy chemistry shows that there are often multiple formation routes for various oxidation products in this reaction. Unfortunately, we are currently unable to quantify the branching ratio for these various pathways.

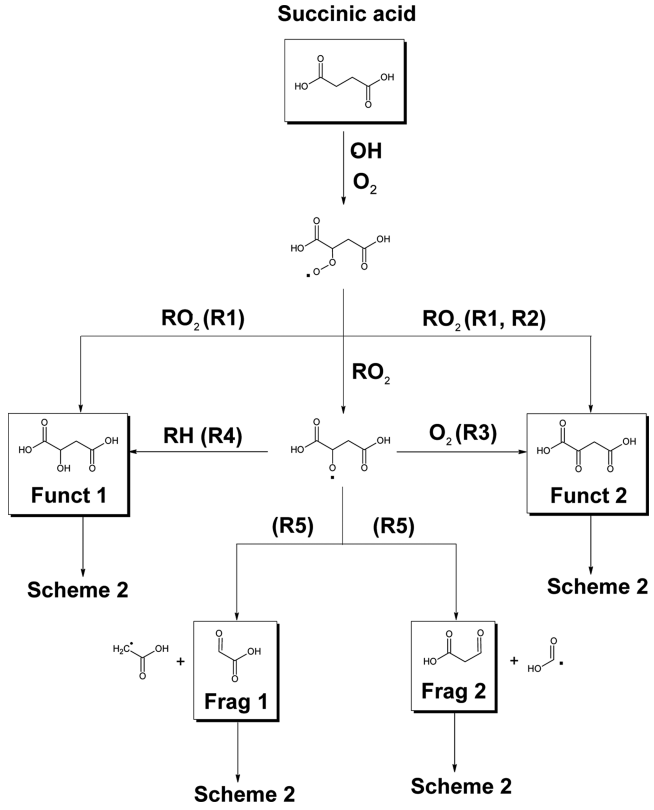

Figure 6. Proposed reaction mechanism for the OH oxidation of succinic acid showing the formation routes of first-generation products. The box indicates the corresponding ion, $[M - H]^-$, that has been detected in the negative mode DART-MS. The reaction numbers (e.g., R1–R5) refer to the general reaction pathways shown in Figure 5.

3.3.2. Second-Generation Products. Products of the first-generation reaction described above (both functionalization and fragmentation) can be further oxidized by OH radicals to form the second-generation species shown in Figure 7. The boxes in Figure 7 show reaction products detected via DART and shown in Tables 2 and 3. The reaction of OH radicals with different H abstraction sites on the first-generation products can lead to a variety of products. For malic acid (Funct 1), H atom abstraction from the secondary carbon (Path 1, Figure 7), followed by a peroxy self-reaction, can produce tartaric acid (Funct 3) and 2-hydroxy-3-oxosuccinic acid (Funct 4). The peroxy self-reaction could also produce two alkoxy radicals that form glyoxylic acid (Frag 1) and 2-hydroxy-3-oxopropanoic acid (Frag 3) after C–C bond scission.

If the OH radical abstracts the H atom from the tertiary carbon site (Path 2, Figure 7) of malic acid, only an alcohol functional group can be formed at this tertiary carbon, thus producing 2,2-dihydroxysuccinic acid (Funct 5). Oxalic acid (Frag 4) and malonic acid (Frag 5), two smaller dicarboxylic acids, can be formed through the decomposition of the alkoxy radical formed at this tertiary carbon site.

Oxosuccinic acid (Funct 2) has two aliphatic H atoms on a secondary carbon available for H abstraction by OH radicals (Path 3, Figure 7) to eventually form 2-hydroxy-3-oxosuccinic acid (Funct 4). Although 2,3-dioxosuccinic acid can be potentially formed through functionalization, it is not observed in the DART mass spectra for either aerosol phase. Two smaller monoacids (glyoxylic acid (Frag 1) and 2,3-

dx.doi.org/10.1021/jp5012022 | J. Phys. Chem. C 2014, 118, 28978–28992

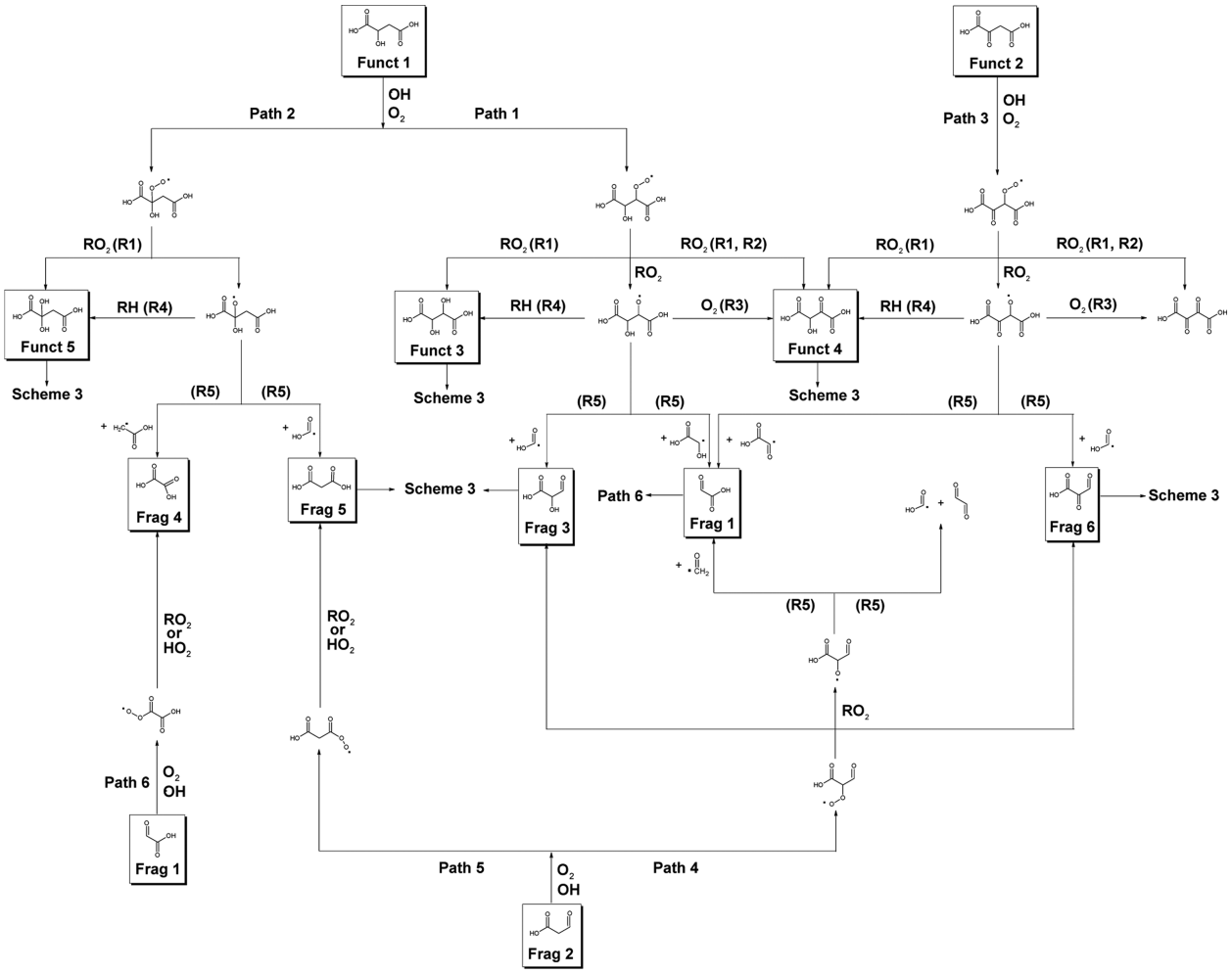

Figure 7. Proposed reaction mechanism for the oxidation of first-generation products. The box indicates the corresponding ion, $[M - H]^-$, has been detected in the negative mode DART-MS. The reaction numbers (e.g., R1−R5) refer to the general reaction pathways shown in Figure 5.

dioxopropanoic acid (Frag 6)) can be formed by fragmentation. For the two first-generation fragmentation products, they can be functionalized or fragmented (Paths 4−6) to yield the second-generation fragmentation products (Frag 1, 3−6), which can also be generated through the fragmentation of the first-generation functionalization products (Funct 1 and Funct 2).

3.3.3. Third-Generation Products. Figure 8 shows the subsequent OH oxidation of the second-generation products. When the oxidation proceeds, based on detected ions in the mass spectra, C−C bond scission reactions (**R5** in Figure 5) of the second-generation functionalization products appear to be most favorable. For example, the $C_4H_5O_7^-$ ion corresponding to the addition of an alcohol functional group to tartaric acid (Funct 3) is not observed. Instead, as the second-generation functionalization products (Funct 3, 4, and 5) react with OH, they likely undergo exclusively carbon bond scission to produce the observed products in our mass spectrum. For example, when the H atom from the secondary carbon of 2,2-dihydroxysuccinic acid (Funct 5) is abstracted by the OH radical (Path 7, Figure 8), it fragments to yield glyoxylic acid (Frag 1) and 2,2-dihydroxy-3-oxopropanoic acid (Frag 7). For tartaric acid (Funct 4, Path 8) and 2-hydroxy-3-oxosuccinic acid (Funct 5, Path 9 in Figure 8), when the H atom from the tertiary carbon is removed, a peroxy radical is formed at the tertiary site, which can subsequently fragment to yield smaller diacids (oxalic acid (Frag 4), hydroxymalonic acid (Frag 8), and oxomalonic acid (Frag 9)). The third-generation fragmentation products can also be produced from the oxidation of the second-generation fragmentation products via Paths 10−13 in Figure 8. For example, as depicted in Path 12 (Figure 8), the oxidation of malonic acid (Frag 5) leads to hydroxymalonic acid (Frag 8) and oxomalonic acid (Frag 9) through the functionalization.

3.3.4. Kinetic Evolution of Oxidation Products. Functionalization and fragmentation products as a group evolve with the OH exposure in markedly different ways. In the solid aerosol (Figure 3) at all OH exposures, the product yields are small. Both functionalization (Figure 3B) and fragmentation (Figure 3C) products are observed to increase at nearly the same rate with increasing OH exposure. At the end of the reaction the aerosol is comprised of ∼8% of fragmentation products and less than a percent of functionalization products. The dominant reaction product is oxalic acid, accounting for nearly 4% of the total aerosol mass at the end of the reaction. The remaining fraction (∼90%) of the solid aerosol is succinic acid.

In contrast, a distinct kinetic pattern is observed for the functionalization and fragmentation products in aqueous droplets (Figure 4). For functionalization products (Figure 4B), the first-generation products (Funct 1 and Funct 2) reach a maximum concentration (about 2% of total ion signal) at an OH exposure of 0.5×10^{12} molecules cm^{-3} s. Their

dx.doi.org/10.1021/jp5012022 | J. Phys. Chem. C 2014, 118, 28978−28992

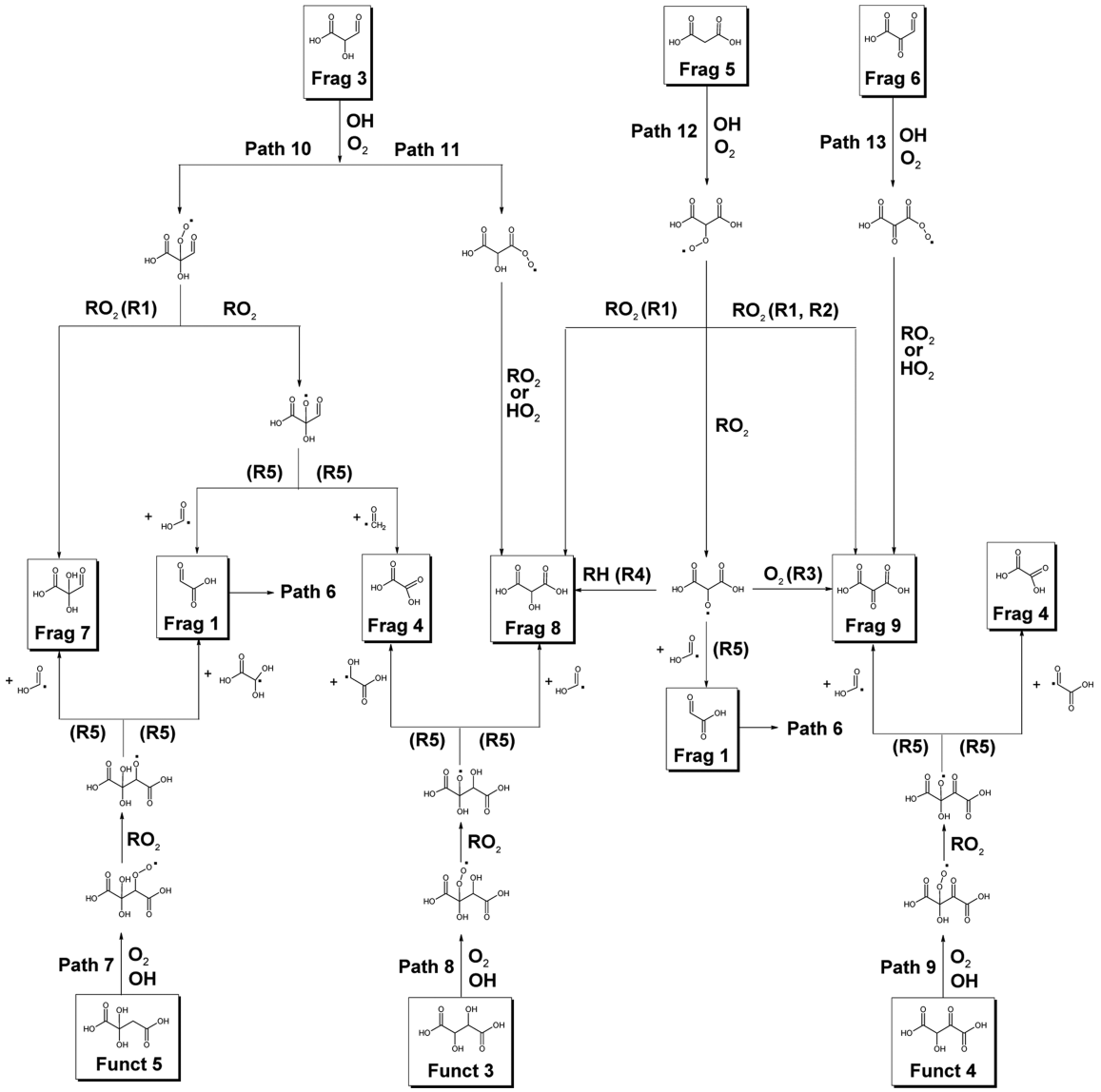

Figure 8. Proposed reaction mechanisms for the oxidation of second-generation products. The box indicates the corresponding ion, $[M - H]^-$, has been detected in the negative mode DART-MS. The reaction numbers (e.g., R1−R5) refer to the general reaction pathways shown in Figure 5.

concentration then decreases with increasing OH exposure, approaching zero at the highest OH exposures accessed in the experiment. The concentration of second-generation products (Funct 3, 4, 5) follow a different kinetic evolution than the first-generation products and reach their maximum value at larger OH exposures (OH exposure > 1.6×10^{12} molecules cm^{-3} s). This kinetic trend is consistent with the formation of second-generation products from the reaction of OH with first-generation species and is consistent with the multigenerational reaction shown in Figures 6 and 7.

In contrast, the fragmentation products exhibit a much more complex kinetic evolution indicating that they are likely formed from generations 1 thru 3 (Figure 4C). This is explained in part by multiple oxidation routes leading to the same fragmentation products as shown in Figures 6−8. For example, glyoxylic acid (Frag 1) is a common fragmentation product, which can be formed by independent reaction pathways in each of the first three generations. The chemical evolution of the oxidation products thus provides further qualitative evidence to support the proposed reaction mechanisms and product assignments presented above.

In general, Figures 3 and 4 reveal that the fragmentation products are much more abundant than functionalization products. Although the yields are small in solid aerosols, as shown in Figure 3D, the total concentration of fragmentation products (2−8%) is larger than the total functionalization products, which accounts for less than 0.2% of the aerosol over the course of the reaction. For aqueous droplets (Figure 4D), at higher oxidation levels (OH exposure >0.5×10^{12} molecules cm^{-3} s), the oxidation products, especially fragmentation products, contribute significantly to the aerosol mass. At the highest OH exposure, the fragmentation products comprise 70% of the aerosol compared with the functionalization products which are less than 2% (Figure 4D).

Among the observed products, hydroxymalonic acid (Frag 9, $C_3H_2O_5$) is the most abundant species, accounting for 30% of the total particle signal. Oxalic acid (Frag 4, $C_2H_2O_4$) and glyoxylic acid (Frag 1, $C_2H_2O_3$) are other major species, contributing about 20% and 15% of the total ion signal,

dx.doi.org/10.1021/jp5012022 | J. Phys. Chem. C 2014, 118, 28978−28992

respectively. These three major fragmentation products are formed at higher oxidation stages (Table 3). Together these observations suggest that the relative importance of fragmentation versus functionalization increases with increasing oxidation levels.

Gas-phase products of the reaction are measured by passing the aerosol stream exiting the flow reactor through a filter, which was used to remove the aerosol. After removing background ions originating from the ion source from the gas-phase mass spectra, a weak signal of one ion (m/z 89.89) with a suggested formula of $C_2H_2O_4$ is positively identified in the gas phase for both solid aerosols and aqueous droplets. The intensity of the ion signal is about 10−20% larger than the background signal. The gas-phase product could be assigned to oxalic acid (Frag 4). This is the only fragmentation product of those detected in the aerosol phase (Table 3) observed in the gas-phase mass spectra. Volatile products such as formaldehyde and CO_2 could be formed in the OH oxidation of succinic acid;[34,41] however, these small molecular weight species would not be detected by the DART mass spectrometer used here.

Overall, the heterogeneous OH oxidation of succinic acid yields a variety of functionalization and fragmentation products after multiple oxidation steps as shown in Figures 6−8. On the basis of the molecular formula of the observed products and the proposed reaction mechanisms, succinic acid preferentially reacts with OH to form small monoacids and dicarboxylic acids. The reaction is also a source for hydroxy- and oxo-substituted monoacids and dicarboxylic acids (Tables 2 and 3). While the schemes presented account for all of the peaks observed in the DART mass spectra, there are several things to note: First, there can be several reaction pathways that lead to identical oxidation products. For example, as shown in Figure 7, oxalic acid (Frag 4) can be formed from the fragmentation of malic acid (Funct 1) through Path 2 as well as from the oxidation of glyoxylic acid (Frag 1) through Path 6. Second, structural isomers of isobaric compounds are most likely formed. For example, depending on whether the H atom from the secondary carbon (Path 1) or tertiary carbon (Path 2) of malic acid (Funct 1) is abstracted by the OH radicals (Figure 7), malic acid can be functionalized to 2,3-dihydroxysuccinic acid (tartaric acid, Funct 3) and 2,2-dihydroxysuccinic acid (Funct 5). These two structural isomers have the same chemical formula ($C_4H_6O_6$) and cannot be differentiated in our mass spectrometer.

For isobaric compounds, as shown in Figure 7, the fragmentation of malic acid (Funct 1) can lead to malonic acid (Frag 5, a dicarboxylic acid) (Path 2) and 2-hydroxy-3-oxopropanoic acid (Frag 3, a monoacid) (Path 1). Again, these two isobaric compounds ($C_3H_4O_4$) cannot be differentiated. Therefore, unique oxidation products cannot be easily assigned for a specific reaction pathway. Without knowing the rate constants for individual reactions, we thus do not attempt to assign branching ratios for different oxidation pathways based on the observed products. Although the individual branching ratios cannot be determined, the concentration of fragmentation products is clearly much larger than that of functionalization products for both phases, suggesting that the fragmentation is the dominant reaction pathway upon oxidation.

Higher-generation functionalization products (e.g., third or higher generations) are not observed in mass spectra. Oxidation of second-generation functionalization products (Funct 3, 4, and 5) exclusively undergoes C−C bond scission reactions to yield the observed products, as shown in Figure 8. This observation is consistent with the hypothesis that the fragmentation becomes more favorable than functionalization for highly oxygenated hydrocarbons.[14,15,20] Although higher-generation products (e.g., fourth or higher generations) are not observed in the DART mass spectra at the highest OH exposure for both phases, it is not surprising that the third-generation products can be further oxidized. For example, the oxidation of oxalic acid (Frag 4) in aqueous droplets can lead to the formation of CO_2, which will escape to the gas phase and not be detected by DART.[34] This may in part explain the changes in aerosol volume observed in both phases.

3.4. Average Aerosol Elemental Composition. From the relative intensity and the molecular formulas of the oxidation products, the average change in aerosol elemental composition with OH exposure is computed. The relative population of succinic acid and its oxidation products in the particle are quantified after correcting for the relative ionization efficiencies (as discussed in the Experimental Section). Some uncertainty in this analysis is introduced given the limited set of authentic standards. The goal of this analysis is to better understand how the molecular distribution of oxidation products ultimately controls the bulk average elemental (e.g., ⟨O/C⟩) aerosol composition, a key metric that is now commonly measured and used to quantify aerosol oxidation reactions.[43−46] The average oxygen-to-carbon (⟨O/C⟩) and hydrogen-to-carbon (⟨H/C⟩) ratios of the aerosol are

$$\left\langle \frac{O}{C} \right\rangle = \sum_i (O/C)_i I_i \tag{6}$$

$$\left\langle \frac{H}{C} \right\rangle = \sum_i (H/C)_i I_i \tag{7}$$

where $(O/C)_i$, $(H/C)_i$, and I_i are the O/C, H/C, and relative abundance of oxidation product i, respectively. As shown in Tables 2 and 3, the O/C_i and H/C_i ratios of the observed products range from 1 to 2 and 0.5 to 1.33, respectively. A van Krevelen plot is used to represent the oxidation of succinic acid as a function of OH exposure (Figure 9). For solid aerosol and aqueous droplets, when the OH exposure increases, the ⟨O/C⟩ increases, while the ⟨H/C⟩ decreases. The slope of the line for

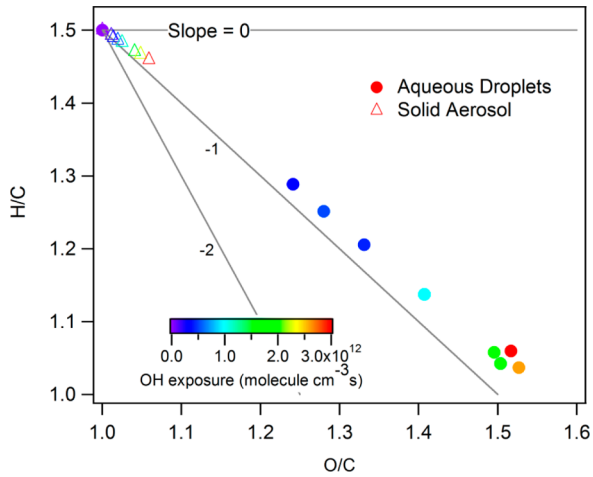

Figure 9. van Krevelen diagram for the heterogeneous OH oxidation of succinic acid aerosols in solid (triangle) and aqueous phases (circle) as a function of OH exposure.

dx.doi.org/10.1021/jp5012022 | J. Phys. Chem. C 2014, 118, 28978−28992

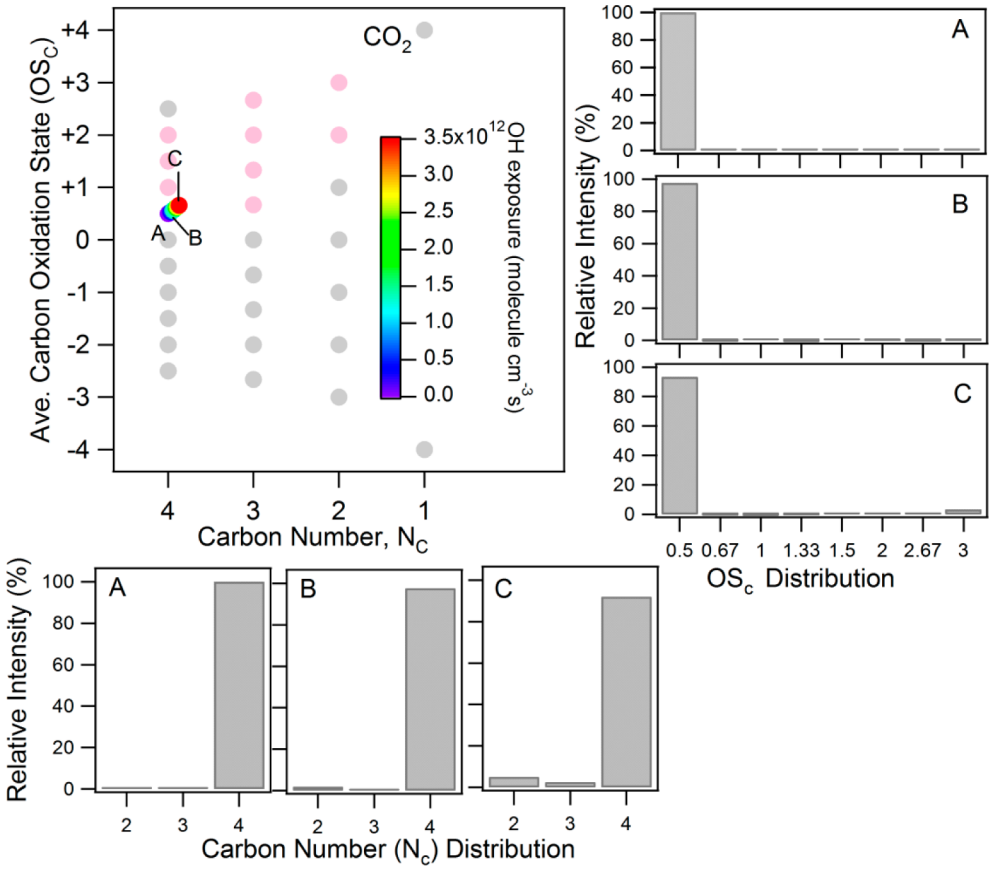

Figure 10. Heterogeneous OH oxidation of solid succinic acid aerosols represented in average aerosol $\langle OS_C \rangle$ vs $\langle N_C \rangle$ space (see text for details). The pink circles are the observed oxidation products. Molecular distributions of OS_C (right) and N_C (bottom) are shown at OH exposures of (A) 0, (B) 3.9×10^{11} molecules cm^{-3} s, and (C) 2.5×10^{12} molecules cm^{-3} s.

aqueous droplets (-0.88 ± 0.02) is slightly steeper than that of solid aerosol (-0.70 ± 0.01). Although the slopes of the lines in the van Krevelen plot are very similar for both phases, there is a significant difference in the extent of oxidation that is observed. For solid aerosol, the change in $\langle O/C \rangle$ ($\langle \Delta O/C \rangle$ = 0.05) and $\langle H/C \rangle$ ($\langle \Delta H/C \rangle$ = −0.04) is very small at the highest OH exposure since the aerosols are mainly composed of unreacted succinic acid (cf. Figure 3A). A dramatic change in $\langle O/C \rangle$ and $\langle H/C \rangle$ ratios is observed for aqueous droplets. At the highest OH exposure, the $\langle O/C \rangle$ increases from 1.0 to 1.52, and the $\langle H/C \rangle$ drops from 1.50 to 1.06. The increase in the $\langle O/C \rangle$ ratio is consistent with the functionalization and fragmentation products shown in Tables 2 and 3. The decrease in the $\langle H/C \rangle$ ratio is attributed to both the formation of new carbonyl functional groups and smaller molecular weight acids (glyoxylic acid, Frag 1, and oxalic acid, Frag 4) produced by C−C bond scission.

3.4.2. Average Aerosol Carbon Oxidation State vs Carbon Number. The elemental ratios described above can be used to compute an oxidation trajectory in average aerosol carbon oxidation state ($\langle OS_C \rangle$) and carbon number ($\langle N_C \rangle$) space.[12,14,16] This representation enables a closer inspection of how the underlying molecular distribution of individual products ultimately governs the average oxidative evolution of the aerosol. The average carbon oxidation state ($\langle OS_c \rangle$) and carbon number ($\langle N_C \rangle$) are computed as follows

$$\langle OS_C \rangle = \sum_i \left(2\frac{O}{C} - \frac{H}{C}\right)_i I_i \quad (8)$$

$$\langle N_C \rangle = \sum_i (N_C)_i I_i \quad (9)$$

where (O/C) and (H/C) are the O/C and H/C ratios computed of product i at a given OH exposure. $(N_C)_i$ is the carbon number of oxidation product i. The OS_C and N_C of the oxidation products range from 2 to 4 and 0.5 to 3, respectively (Tables 2 and 3).

For the solid aerosol (Figure 10), $\langle OS_C \rangle$ increases only slightly from 0.5 to 0.65, while the average aerosol $\langle N_C \rangle$ decreases from 4.0 to 3.89. Also shown in Figure 10 is the OS_C and carbon number distributions of individual molecular products. As observed above, the oxidation state of the solid aerosol over a broad range of experimental OH exposures is mainly controlled by the persistent quantity of unreacted succinic acid (OS_C = 0.5, N_C =4), which contributes to more than 90% of the aerosol mass. The slight increase in $\langle OS_C \rangle$ and decrease in $\langle N_C \rangle$ is due almost entirely to the production (less than a 10%) of C_2 fragmentation products (Figure 3C), such as oxalic acid (OS_C = 3, N_C = 2) formed during the reaction.

For aqueous droplets (Figure 11) the $\langle OS_C \rangle$ increases from 0.5 to 2.01, while $\langle N_C \rangle$ decreases from 4.0 to 2.94 at the highest OH exposures. Upon oxidation the abundance of succinic acid (C_4, OS_C = 0.5) decreases dramatically from 100% to about 20%, with the dominant C_4 species in the aerosol at all oxidation levels being succinic acid. Alternatively, the concentration of C_2 and C_3 fragmentation products increases with OH exposure, contributing more than 50% of total aerosol mass at the end of the reaction. During much of the reaction

dx.doi.org/10.1021/jp5012022 | J. Phys. Chem. C 2014, 118, 28978−28992

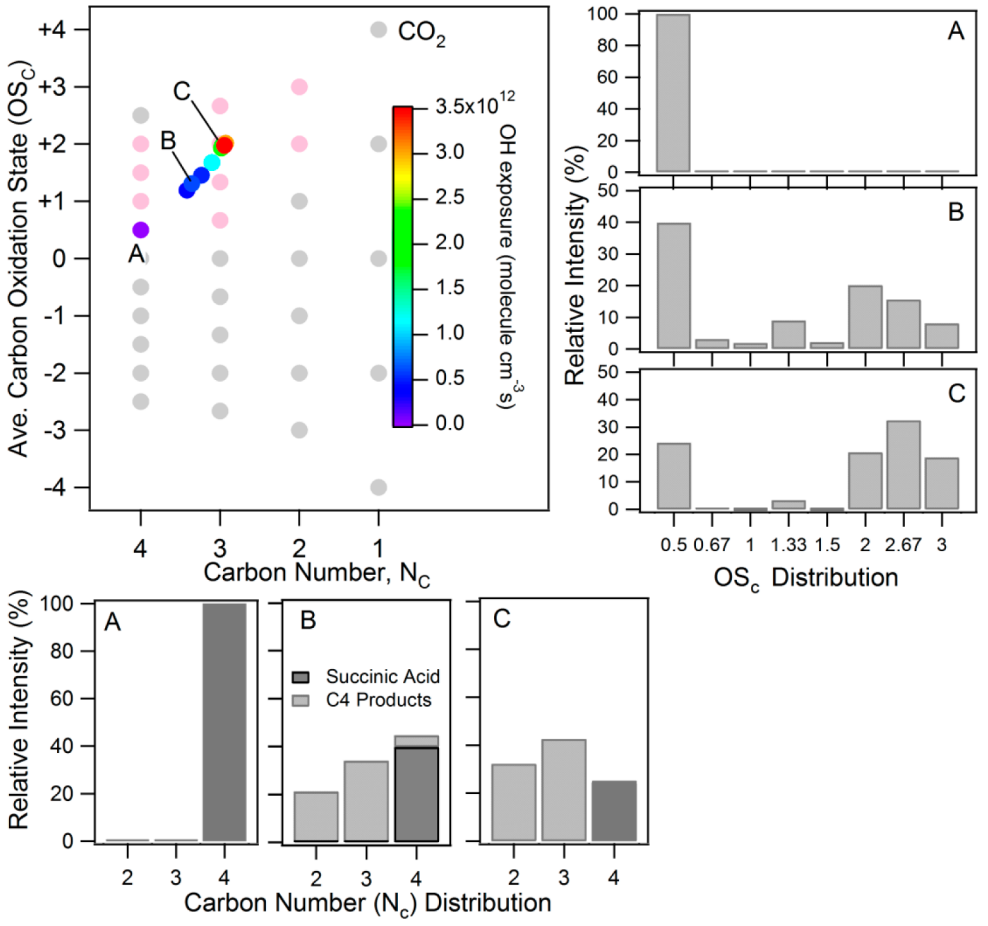

Figure 11. Heterogeneous OH oxidation of aqueous succinic acid droplets represented in average aerosol $\langle OS_C \rangle$ vs $\langle N_C \rangle$ space (see text for details). The pink circles are the observed oxidation products. Molecular distributions of OS_C (right) and N_C (bottom) are shown at OH exposures of (A) 0, (B) 3.6×10^{11} molecules cm^{-3} s, and (C) 2.2×10^{12} molecules cm^{-3} s.

there is a bimodal distribution (neglecting the contribution of succinic acid) in molecular oxidation states, with modes centered at OS_C = 1.33 and 2.67. At intermediate exposures ([OH]t = 3.6×10^{11} molecules cm^{-3} s, B in Figure 11) C_4 functionalization products malic acid (Funct 1, OS_C = 1), oxosuccinic acid (Funct 2, OS_C = 1.5), tartaric acid (Funct 3, OS_C = 1.5), 2-hydroxy-3-oxosuccinic acid (Funct 4, OS_C = 2), and 2-hydroxy-2-oxosuccinic acid (Funct 5 OS_C = 2) account for the small cluster of oxidation states centered about 1.33. The peak itself at OS_C = 1.33 corresponds to two dominant fragmentation products 2-hydroxy-3-oxopropanoic acid (Frag 3, OS_C = 1.33) and malonic acid (Frag 5, OS_C = 1.33).

During much of the reaction, products having an $OS_C \geq 2$ and carbon numbers less than 4 are the most abundant aqueous aerosol species and thus contribute most to the observed changes in average aerosol oxidation state and carbon number. The fragmentation species that dominate the distribution are oxomalonic acid (Frag 9, N_C = 3, OS_c = 2.67), glyoxylic acid (Frag 1, N_C = 2, OS_c = 2), and oxalic acid (Frag 4, N_C = 2, OS_C = 3). These results clearly show that the oxidative evolution of the $\langle OS_C \rangle$ and $\langle N_C \rangle$ of aqueous droplets is controlled by the underlying distribution of fragmentation products with high carbon oxidation states. This is in contrast with chemical reduced organic aerosol, whose average aerosol carbon oxidation state is controlled by a Poisson distribution of functionalization products as previously shown by Wilson et al.[14]

4. CONCLUSIONS

The heterogeneous OH oxidation of succinic acid in solid and aqueous phases is investigated using an aerosol flow tube reactor. The molecular formula of the aerosol oxidation products is determined using a soft atmospheric pressure ionization source (DART) coupled with a high-resolution mass spectrometer. While there are similarities in the identity of the oxidation products observed in the DART mass spectra of solid and aqueous aerosol, there are significant differences in the reaction kinetics of succinic acid and the chemical evolution of products for the two phases, suggesting that the aerosol phase plays an important role in oxidation. Kinetic measurements show that succinic acid decays much faster, ~41 times faster, in aqueous droplets than in solid aerosol. Significant concentrations have been observed for the oxidation products in aqueous droplets, contributing more than 70% of the aerosol mass at high OH exposures. The differences between solid and aqueous aerosol can be explained by the more rapid diffusion (early on in the reaction) of aqueous succinic acid and its oxidation products to the aerosol surface for reaction with OH. The reactive OH uptake efficiency is estimated to be about 1.65 for aqueous droplets, suggesting the presence of radical chain chemistry (e.g., alkoxy radical abstraction pathways). Together these results point more generally to the potential complexity of aerosol oxidation in the atmosphere, which may depend greatly on "exposure history" of the aerosol to fluctuations in

dx.doi.org/10.1021/jp5012022 | J. Phys. Chem. C 2014, 118, 28978−28992

relative humidity, temperature, liquid water content, or other factors that control phase.

On the basis of the molecular analysis presented here, succinic acid reacts with OH (in the presence of O_2) to form primarily smaller carbon number monoacids and dicarboxylic acids (e.g., oxalic acid and malonic acid). The observed products are explained by the well-known pathways such as the Russell, Bennett and Summers, and alkoxy radical reaction mechanisms. Upon oxidation of the aqueous aerosol, the concentration of fragmentation products (C_2 and C_3) increases with increasing OH exposure, while the C_4 functionalization products initially form in small quantities and decrease as oxidation progresses suggesting that C−C bond scission reactions dominate the oxidation chemistry at higher generations. The high concentration of fragmentation products formed during this reaction is consistent with fragmentation pathways becoming dominant for more oxygenated molecular species (i.e., O/C > 0.5).[15,16] Overall, aerosol water content is found to play a controlling role in both the speed and extent of aerosol oxidation as shown through the molecular evolution of oxidation products and the average aerosol carbon number and oxidation state. Generally, these results point to the importance of understanding coupled reaction−diffusion processes in formation and chemical aging of organic aerosol.

AUTHOR INFORMATION

Corresponding Author

*E-mail: krwilson@lbl.gov. Phone: 510-495-2474.

Notes

The authors declare no competing financial interest.

ACKNOWLEDGMENTS

This work is supported by the Department of Energy's Office of Science Early Career Research Program and by the Director, Office of Energy Research, Office of Basic Energy Sciences, Chemical Sciences, Geosciences, and Biosciences Division of the U.S. Department of Energy under Contract No. DE-AC02-05CH11231. H.Z. is funded by the Dreyfus Foundation Postdoctoral Fellowship Program.

REFERENCES

(1) Hallquist, M.; Wenger, J. C.; Baltensperger, U.; Rudich, Y.; Simpson, D.; Claeys, M.; Dommen, J.; Donahue, N. M.; George, C.; Goldstein, A. H.; et al. The Formation, Properties and Impact of Secondary Organic Aerosol: Current and Emerging Issues. *Atmos. Chem. Phys.* **2009**, *9* (14), 5155−5236.

(2) George, I. J.; Abbatt, J. P. D. Heterogeneous Oxidation of Atmospheric Aerosol Particles by Gas-Phase Radicals. *Nature Chem.* **2010**, *2* (9), 713−722.

(3) Kessler, S. H.; Smith, J. D.; Che, D. L.; Worsnop, D. R.; Wilson, K. R.; Kroll, J. H. Chemical Sinks of Organic Aerosol: Kinetics and Products of the Heterogeneous Oxidation of Erythritol and Levoglucosan. *Environ. Sci. Technol.* **2010**, *44* (18), 7005−7010.

(4) Slade, J. H.; Knopf, D. A. Heterogeneous OH Oxidation of Biomass Burning Organic Aerosol Surrogate Compounds: Assessment of Volatilisation Products and the Role of Oh Concentration on the Reactive Uptake Kinetics. *Phys. Chem. Chem. Phys.* **2013**, *15* (16), 5898−5915.

(5) Lambe, A. T.; Zhang, J.; Sage, A. M.; Donahue, N. M. Controlled OH Radical Production Via Ozone-Alkene Reactions for Use in Aerosol Aging Studies. *Environ. Sci. Technol.* **2007**, *41* (7), 2357−2363.

(6) Weitkamp, E. A.; Lambe, A. T.; Donahue, N. M.; Robinson, A. L. Laboratory Measurements of the Heterogeneous Oxidation of Condensed-Phase Organic Molecular Makers for Motor Vehicle Exhaust. *Environ. Sci. Technol.* **2008**, *42* (21), 7950−7956.

(7) George, I. J.; Chang, R. Y. W.; Danov, V.; Vlasenko, A.; Abbatt, J. P. D. Modification of Cloud Condensation Nucleus Activity of Organic Aerosols by Hydroxyl Radical Heterogeneous Oxidation. *Atmos. Environ.* **2009**, *43* (32), 5038−5045.

(8) Harmon, C. W.; Ruehl, C. R.; Cappa, C. D.; Wilson, K. R. A Statistical Description of the Evolution of Cloud Condensation Nuclei Activity During the Heterogeneous Oxidation of Squalane and Bis(2-Ethylhexyl) Sebacate Aerosol by Hydroxyl Radicals. *Phys. Chem. Chem. Phys.* **2013**, *15* (24), 9679−9693.

(9) George, I. J.; Vlasenko, A.; Slowik, J. G.; Broekhuizen, K.; Abbatt, J. P. D. Heterogeneous Oxidation of Saturated Organic Aerosols by Hydroxyl Radicals: Uptake Kinetics, Condensed-Phase Products, and Particle Size Change. *Atmos. Chem. Phys.* **2007**, *7* (16), 4187−4201.

(10) Hearn, J. D.; Renbaum, L. H.; Wang, X.; Smith, G. D. Kinetics and Products from Reaction of Cl Radicals with Dioctyl Sebacate (Dos) Particles in O2: A Model for Radical-Initiated Oxidation of Organic Aerosols. *Phys. Chem. Chem. Phys.* **2007**, *9* (34), 4803−4813.

(11) McNeill, V. F.; Yatavelli, R. L. N.; Thornton, J. A.; Stipe, C. B.; Landgrebe, O. Heterogeneous Oh Oxidation of Palmitic Acid in Single Component and Internally Mixed Aerosol Particles: Vaporization and the Role of Particle Phase. *Atmos. Chem. Phys.* **2008**, *8* (17), 5465−5476.

(12) Mysak, E. R.; Smith, J. D.; Ashby, P. D.; Newberg, J. T.; Wilson, K. R.; Bluhm, H. Competitive Reaction Pathways for Functionalization and Volatilization in the Heterogeneous Oxidation of Coronene Thin Films by Hydroxyl Radicals and Ozone. *Phys. Chem. Chem. Phys.* **2011**, *13* (16), 7554−7564.

(13) Smith, J. D.; Kroll, J. H.; Cappa, C. D.; Che, D. L.; Liu, C. L.; Ahmed, M.; Leone, S. R.; Worsnop, D. R.; Wilson, K. R. The Heterogeneous Reaction of Hydroxyl Radicals with Sub-Micron Squalane Particles: A Model System for Understanding the Oxidative Aging of Ambient Aerosols. *Atmos. Chem. Phys.* **2009**, *9* (9), 3209−3222.

(14) Wilson, K. R.; Smith, J. D.; Kessler, S. H.; Kroll, J. H. The Statistical Evolution of Multiple Generations of Oxidation Products in the Photochemical Aging of Chemically Reduced Organic Aerosol. *Phys. Chem. Chem. Phys.* **2012**, *14* (4), 1468−1479.

(15) Kroll, J. H.; Smith, J. D.; Che, D. L.; Kessler, S. H.; Worsnop, D. R.; Wilson, K. R. Measurement of Fragmentation and Functionalization Pathways in the Heterogeneous Oxidation of Oxidized Organic Aerosol. *Phys. Chem. Chem. Phys.* **2009**, *11* (36), 8005−8014.

(16) Kroll, J. H.; Donahue, N. M.; Jimenez, J. L.; Kessler, S. H.; Canagaratna, M. R.; Wilson, K. R.; Altieri, K. E.; Mazzoleni, L. R.; Wozniak, A. S.; Bluhm, H.; et al. Carbon Oxidation State as a Metric for Describing the Chemistry of Atmospheric Organic Aerosol. *Nature Chem.* **2011**, *3* (2), 133−139.

(17) Ruehl, C. R.; Nah, T.; Isaacman, G.; Worton, D. R.; Chan, A. W. H.; Kolesar, K. R.; Cappa, C. D.; Goldstein, A. H.; Wilson, K. R. The Influence of Molecular Structure and Aerosol Phase on the Heterogeneous Oxidation of Normal and Branched Alkanes by Oh. *J. Phys. Chem. A* **2013**, *117* (19), 3990−4000.

(18) Saxena, P.; Hildemann, L. M. Water-Soluble Organics in Atmospheric Particles: A Critical Review of the Literature and Application of Thermodynamics to Identify Candidate Compounds. *J. Atmos. Chem.* **1996**, *24* (1), 57−109.

(19) Goldstein, A. H.; Galbally, I. E. Known and Unexplored Organic Constituents in the Earth's Atmosphere. *Environ. Sci. Technol.* **2007**, *41* (5), 1514−1521.

(20) Jimenez, J. L.; Canagaratna, M. R.; Donahue, N. M.; Prevot, A. S. H.; Zhang, Q.; Kroll, J. H.; DeCarlo, P. F.; Allan, J. D.; Coe, H.; Ng, N. L.; et al. Evolution of Organic Aerosols in the Atmosphere. *Science* **2009**, *326* (5959), 1525−1529.

(21) Kessler, S. H.; Nah, T.; Daumit, K. E.; Smith, J. D.; Leone, S. R.; Kolb, C. E.; Worsnop, D. R.; Wilson, K. R.; Kroll, J. H. OH-Initiated Heterogeneous Aging of Highly Oxidized Organic Aerosol. *J. Phys. Chem. A* **2012**, *116* (24), 6358−6365.

(22) Hennigan, C. J.; Sullivan, A. P.; Collett, J. L.; Robinson, A. L. Levoglucosan Stability in Biomass Burning Particles Exposed to Hydroxyl Radicals. *Geophys. Res. Lett.* **2010**, *37*, L09806.
(23) Hearn, J. D.; Smith, G. A. Ozonolysis of Mixed Oleic Acid/N-Docosane Particles: The Roles of Phase, Morphology, and Metastable States. *J. Phys. Chem. A* **2007**, *111* (43), 11059−11065.
(24) Renbaum, L. H.; Smith, G. D. The Importance of Phase in the Radical-Initiated Oxidation of Model Organic Aerosols: Reactions of Solid and Liquid Brassidic Acid Particles. *Phys. Chem. Chem. Phys.* **2009**, *11* (14), 2441−2451.
(25) Renbaum, L. H.; Smith, G. D. Organic Nitrate Formation in the Radical-Initiated Oxidation of Model Aerosol Particles in the Presence of Nox. *Phys. Chem. Chem. Phys.* **2009**, *11* (36), 8040−8047.
(26) Santarpia, J. L.; Li, R. J.; Collins, D. R. Direct Measurement of the Hydration State of Ambient Aerosol Populations. *J. Geophys. Res., [Atmos.]* **2004**, *109* (D18), D18209.
(27) Taylor, N. F.; Collins, D. R.; Spencer, C. W.; Lowenthal, D. H.; Zielinska, B.; Samburova, V.; Kumar, N. Measurement of Ambient Aerosol Hydration State at Great Smoky Mountains National Park in the Southeastern United States. *Atmos. Chem. Phys.* **2011**, *11* (23), 12085−12107.
(28) Crank, J.; Park, G. S. *Diffusion in Polymers*; John Wiley and Sons: London, 1968.
(29) Lee, J. W. L.; Carrascon, V.; Gallimore, P. J.; Fuller, S. J.; Bjoerkegren, A.; Spring, D. R.; Pope, F. D.; Kalberer, M. The Effect of Humidity on the Ozonolysis of Unsaturated Compounds in Aerosol Particles. *Phys. Chem. Chem. Phys.* **2012**, *14* (22), 8023−8031.
(30) Najera, J. J.; Percival, C. J.; Horn, A. B. Kinetic Studies of the Heterogeneous Oxidation of Maleic and Fumaric Acid Aerosols by Ozone under Conditions of High Relative Humidity. *Phys. Chem. Chem. Phys.* **2010**, *12* (37), 11417−11427.
(31) Gallimore, P. J.; Achakulwisut, P.; Pope, F. D.; Davies, J. F.; Spring, D. R.; Kalberer, M. Importance of Relative Humidity in the Oxidative Ageing of Organic Aerosols: Case Study of the Ozonolysis of Maleic Acid Aerosol. *Atmos. Chem. Phys.* **2011**, *11* (23), 12181−12195.
(32) Chan, M. N.; Nah, T.; Wilson, K. R. Real Time in Situ Chemical Characterization of Sub-Micron Organic Aerosols Using Direct Analysis in Real Time Mass Spectrometry (Dart-Ms): The Effect of Aerosol Size and Volatility. *Analyst* **2013**, *138* (13), 3749−3757.
(33) Nah, T.; Chan, M.; Leone, S. R.; Wilson, K. R. Real Time in Situ Chemical Characterization of Submicrometer Organic Particles Using Direct Analysis in Real Time-Mass Spectrometry. *Anal. Chem.* **2013**, *85* (4), 2087−2095.
(34) Yang, L.; Ray, M. B.; Yu, L. E. Photooxidation of Dicarboxylic Acids- Part Ii: Kinetics, Intermediates and Field Observations. *Atmos. Environ.* **2008**, *42* (5), 868−880.
(35) Zhang, H.; Ruehl, C. R.; Chan, A. W. H.; Nah, T.; Worton, D. R.; Isaacman, G.; Goldstein, A. H.; Wilson, K. R. Oh-Initiated Heterogeneous Oxidation of Cholestane: A Model System for Understanding the Photochemical Aging of Cyclic Alkane Aerosols. *J. Phys. Chem. A* **2013**, *117* (47), 12449−12458.
(36) Peng, C.; Chan, M. N.; Chan, C. K. The Hygroscopic Properties of Dicarboxylic and Multifunctional Acids: Measurements and Unifac Predictions. *Environ. Sci. Technol.* **2001**, *35* (22), 4495−4501.
(37) Cody, R. B. Observation of Molecular Ions and Analysis of Nonpolar Compounds with the Direct Analysis in Real Time Ion Source. *Anal. Chem.* **2009**, *81* (3), 1101−1107.
(38) Cody, R. B.; Laramee, J. A.; Durst, H. D. Versatile New Ion Source for the Analysis of Materials in Open Air under Ambient Conditions. *Anal. Chem.* **2005**, *77* (8), 2297−2302.
(39) Koop, T.; Bookhold, J.; Shiraiwa, M.; Poeschl, U. Glass Transition and Phase State of Organic Compounds: Dependency on Molecular Properties and Implications for Secondary Organic Aerosols in the Atmosphere. *Phys. Chem. Chem. Phys.* **2011**, *13* (43), 19238−19255.
(40) Shiraiwa, M.; Ammann, M.; Koop, T.; Poeschl, U. Gas Uptake and Chemical Aging of Semisolid Organic Aerosol Particles. *Proc. Natl. Acad. Sci. U.S.A.* **2011**, *108* (27), 11003−11008.
(41) Gao, S. S.; Abbatt, J. P. D. Kinetics and Mechanism of Oh Oxidation of Small Organic Dicarboxylic Acids in Ice: Comparison to Behavior in Aqueous Solution. *J. Phys. Chem. A* **2011**, *115* (35), 9977−9986.
(42) Leitner, N. K. V.; Dore, M. Hydroxyl Radical Induced Decomposition of Aliphatic Acids in Oxygenated and Deoxygenated Aqueous Solutions. *J. Photochem. Photobiol., A* **1996**, *99* (2−3), 137−143.
(43) Aiken, A. C.; Decarlo, P. F.; Kroll, J. H.; Worsnop, D. R.; Huffman, J. A.; Docherty, K. S.; Ulbrich, I. M.; Mohr, C.; Kimmel, J. R.; Sueper, D.; et al. O/C and Om/Oc Ratios of Primary, Secondary, and Ambient Organic Aerosols with High-Resolution Time-of-Flight Aerosol Mass Spectrometry. *Environ. Sci. Technol.* **2008**, *42* (12), 4478−4485.
(44) Chhabra, P. S.; Flagan, R. C.; Seinfeld, J. H. Elemental Analysis of Chamber Organic Aerosol Using an Aerodyne High-Resolution Aerosol Mass Spectrometer. *Atmos. Chem. Phys.* **2010**, *10* (9), 4111−4131.
(45) Heald, C. L.; Kroll, J. H.; Jimenez, J. L.; Docherty, K. S.; DeCarlo, P. F.; Aiken, A. C.; Chen, Q.; Martin, S. T.; Farmer, D. K.; Artaxo, P. A Simplified Description of the Evolution of Organic Aerosol Composition in the Atmosphere. *Geophys. Res. Lett.* **2010**, *37*, L08803.
(46) Ng, N. L.; Canagaratna, M. R.; Jimenez, J. L.; Chhabra, P. S.; Seinfeld, J. H.; Worsnop, D. R. Changes in Organic Aerosol Composition with Aging Inferred from Aerosol Mass Spectra. *Atmos. Chem. Phys.* **2011**, *11* (13), 6465−6474.